

Development of a cerium-doped lanthanum bromide gamma-ray spectrometer for planetary missions and feasibility studies for determination of elemental abundances of radioactive elements (Th, K and U)

D. K. Panda^{1,2}, D. Banerjee^{1,*}, S. K. Goyal¹,
A. R. Patel¹ and A. D. Shukla¹

¹Planetary Sciences and Exploration Group,
Physical Research Laboratory, Ahmedabad 380 009, India

²Department of Physics, Sardar Patel University,
Vallabh Vidyanagar 388 120, India

We present the development of a cerium-doped lanthanum bromide (LaBr₃:Ce) gamma-ray spectrometer (GRS) with the primary objective of determining the abundance and distribution of Th, U, K, and other major elements, including Fe on the entire planetary surface by measuring gamma-ray signals produced by radioactive decay, neutron inelastic scattering and neutron capture reactions in the energy region 0.03–8 MeV. The energy resolution of the LaBr₃:Ce GRS developed in-house using front-end and processing electronics at 511 and 1274 keV is estimated to be 4.1% and 2.5% respectively. The intrinsic activity count rate for our 3" × 3" LaBr₃:Ce GRS is ~61 counts s⁻¹ (i.e. ~0.18 counts s⁻¹ cm⁻³) for the ⁴⁰K energy window (1400–1520 keV) and ~3.4 counts s⁻¹ for the ²³²Th (2550–2700 keV) energy window. Although this large intrinsic activity of the LaBr₃:Ce crystal inhibits estimation of the concentrations of Th and K, our attempts using a NaI(Tl) GRS (with electronics developed in-house) were more successful. The Th concentration of US-110 was estimated to be ~11.4 ppm and is within 14% of the 13.2 ppm value determined using a HPGe GRS. The K concentration of US-110 was estimated to be 0.87% and is within ~10% of the 0.78% value determined independently using a HPGe GRS.

Keywords: Cerium radioactive elements, gamma ray spectroscopy, lanthanum bromide, sodium iodide.

ELEMENTAL composition of a planetary surface can be deduced from *in situ* measurements or by remote sensing technique and laboratory analysis of returned samples. These techniques have been applied in case of the Moon, while studies of other planets, satellites and asteroids have been carried out using remote sensing technique *in situ* measurements have also been performed in Mars. High energy (>100 keV) gamma-ray spectroscopy is an important technique for remote sensing studies of chemical composition of planetary surfaces, and has been used to

study surface composition of the Moon, Mars and asteroids at various spatial resolutions¹. Here we discuss the development of a cerium-doped lanthanum bromide (LaBr₃:Ce) gamma-ray spectrometer (GRS) for a future planetary orbiter mission. The primary objective is to determine the abundance and distribution of Th, U, K, and other major elements, including Fe on the entire planetary surface by measuring gamma-ray signals produced by radioactive decay, neutron inelastic scattering and neutron capture reactions in the energy region 0.03–8 MeV.

LaBr₃:Ce crystals are the latest among the family of the scintillation counters, and have an advantage over conventional room-temperature detectors^{2–4}. The energy resolution of this detector is 2.8% at 662 keV (¹³⁷Cs) and ~1.6% at 2615 keV (²⁰⁸Tl). The light output of this scintillator is seven times higher in comparison to BGO (Bismuth germanate), and 1.6 times higher compared to NaI(Tl). Furthermore, this detector does not require active or passive cooling systems like HPGe detectors, and can be operated at room temperature. Based on weight, power, and operating temperature considerations for the spacecraft payloads, a LaBr₃:Ce gamma detector appeared to be the best choice for our proposed GRS. However, as outlined below, the gamma-ray background arising from intrinsic activity of ¹³⁸La is significantly large, and makes it difficult to make abundance measurements of Th, U and K in the 0.05–3 MeV energy region. Presently, we have developed a laboratory model of the GRS, using commercial-grade components, which are also available in space-qualified grade. Figure 1 shows the block diagram of the LaBr₃:Ce-based GRS. The development design of the GRS is mainly divided into four parts: (i) front-end electronics; (ii) biasing module; (iii) data processing unit, and (iv) data acquisition system. The front-end electronics mainly consists of a charge-sensitive pre-amplifier, shaping amplifier, discriminator, peak detector and analog-to-digital converter (ADC). The present LaBr₃:Ce detector (BrilLanCe 380)³

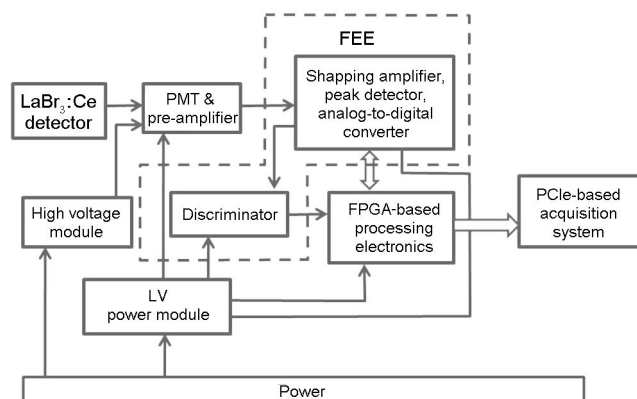


Figure 1. Block diagram of the LaBr₃:Ce gamma-ray spectrometer (GRS).

*For correspondence. (e-mail: deba@prl.res.in)

RESEARCH COMMUNICATIONS

is coupled with a 3.5 inch Photonics 10 stage XP5700 PMT. The GRS design includes a high voltage bias for the PMT to collect the charge.

When a gamma-ray photon interacts with a $\text{LaBr}_3:\text{Ce}$ crystal, the energy of the gamma photon is converted into a light pulse. The scintillation light has a maximum emission at 380 nm, and is converted to electrons in a PMT, which also amplifies the electron current by 5–6 orders of magnitude. The charge pulse is collected by a charge integrating pre-amplifier which generates a voltage pulse whose height is proportional to the energy deposited in the crystal. We have used the pre-amplifier AS2612 module (RC-type) from Saint-Gobain as the charge-sensitive pre-amplifier. The pulse is then shaped (Gaussian) and amplified further by a three-stage (CR-RC²) linear amplifier from a few hundred millivolts to a few volts for A/D conversion. To adjust the pole-zero of the signal, an additional resistance has been used across the capacitor of the first amplifier (CR-amplification stage). We have fixed the threshold voltage to 80 mV, and this configuration will be made variable using a DAC (8-bit). An AMPTEK PH300 peak detector has been used; it is available in hybrid form with high speed, low droop rate and consumes low power. The control logic signals required for peak detector have been generated through FPGA programming. The logic signals are so defined that the peak holds till the ADC conversion time and pulse processing is completed.

The peak detected is digitized using an ADC. We have used a fast 14-bit successive-approximation ADC with a 0.3 μs track/hold acquisition time. The parallel outputs from the ADC are processed by the readout system. The GRS readout system consists of FPGA-based control logic and PCI-based data acquisition card interfaced to the PC with LABVIEW software using a A3P250-

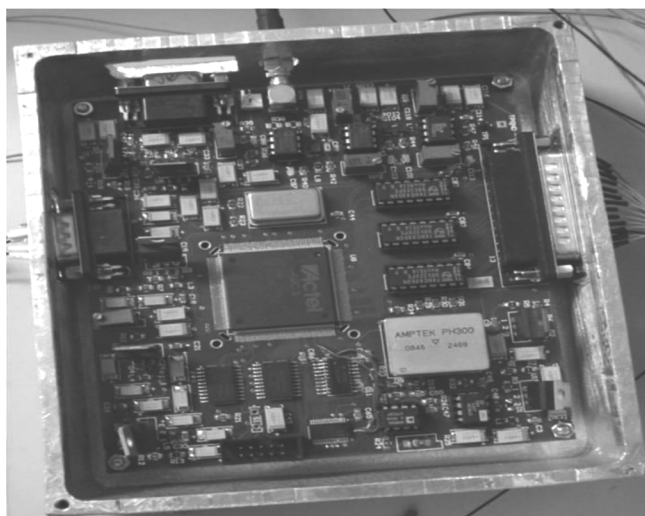


Figure 2. Bread-board model of shaping and processing electronics for the $\text{LaBr}_3:\text{Ce}$ GRS.

PQG208FPGA (Actel, USA). Figure 1 shows the bread-board model and functional block diagrams.

Gamma-ray measurements were carried out using a 3" (diameter) \times 3" (thickness) $\text{LaBr}_3:\text{Ce}$ crystal (BriLanCe 380) coupled to a 3.5 inch photomultiplier (PMT), voltage divider and pre-amplifier procured from Saint-Gobain. The control logic signals and data processed were generated through a FPGA. To improve the signal-to-noise ratio, a single bread-board has been designed consisting of the shaping amplifier, discriminator, peak-detector, ADC and FPGA (Figure 2). Measurement of channel to energy conversion requires analysis of gamma-ray spectra collected and fitting with Gaussian distribution functions for estimation of peak centroid and FWHM. The calibration and photopeak identification have been done using a ^{22}Na radioactive source, and gamma-ray lines arising from the intrinsic activity of ^{138}La (Figure 3). The radioactive source (^{22}Na) is kept in front of the detector at a distance of ~ 15 cm.

Figure 4 shows the proportionality of response, i.e. the linearity curve for the $\text{LaBr}_3:\text{Ce}$ GRS. The energy resolution at 511 and 1274 keV, measured using a ^{22}Na

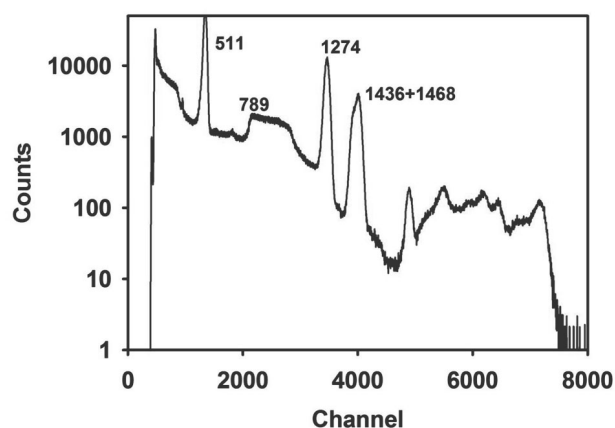


Figure 3. Spectra obtained using the $\text{LaBr}_3:\text{Ce}$ GRS from a ^{22}Na radioactive source.

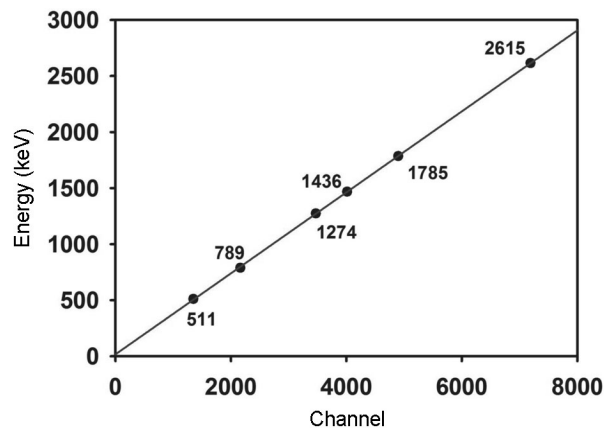


Figure 4. Linearity curve for the $\text{LaBr}_3:\text{Ce}$ GRS.

radioactive source, is 4.1% and 2.5% respectively. The performance of the $\text{LaBr}_3:\text{Ce}$ GRS has been tested and compared with the $\text{NaI}(\text{Tl})$ detector. To achieve a low background, measurements were carried out in a lead shield chamber of 4 inch thickness. Natural lanthanum contains 0.09% of radioactive ^{138}La ($t_{1/2} = 1.05 \times 10^{11}$ years), which decays to produce an excited $^{138}\text{Ce}^*$ during 33.6% of its decay by beta emission, and the remaining 66.4% decay results in the production of excited $^{138}\text{Ba}^*$ by electron capture. $^{138}\text{Ba}^*$ decays by emission of a gamma energy of 1436 keV with a coincident 32 keV X-ray from Ba. Decay of excited ^{138}Ce nuclei occurs by emission of 789 keV gamma ray in coincidence with the beta having an end-point energy of 255 keV. A gamma-ray background spectrum was measured for three days (Figure 5). A pronounced photopeak is observed in the gamma spectrum at ~ 1436 keV, and a Compton continuum from the 789 and 1436 keV gamma-ray peaks. The intrinsic activity count rate for our $\text{LaBr}_3:\text{Ce}$ GRS is 61 counts s^{-1} (i.e. ~ 0.18 counts $\text{s}^{-1} \text{cm}^{-3}$) for the ^{40}K energy window (1400–1520 keV). For the ^{238}U (1700–1800 keV) and ^{232}Th (2550–2700 keV) energy windows, the intrinsic

activity count rates for our detector are ~ 0.37 and ~ 3.4 counts s^{-1} respectively. The measurements using a $2'' \times 2''$ $\text{NaI}(\text{Tl})$ detector showed much lower background values for the above energy windows and consequently, a correction for internal radioactivity is not essential in the analysis of K, Th and U concentrations. The internal radioactivity contributions as obtained from self-counting during background measurement are ~ 0.014 , 0.008 and 0.006 counts s^{-1} for the K, U and Th energy windows respectively.

As a first attempt towards realizing our scientific objectives, we have studied the feasibility of using a $\text{LaBr}_3:\text{Ce}$ GRS for determination of Th, K and U concentrations in soil samples. US-110 is a rock powder standard of basaltic composition prepared in the Physical Research Laboratory, Ahmedabad about 30 years ago. BBS-2 is a red soil collected from southern India. The Th, K and U values for US-110 (Table 1) and BBS-2 have been determined independently using a HPGe GRS⁵. Using the 1400–1520 keV and 2550–2700 keV energy windows, we estimated the K and Th concentrations of US-110, using KCl and BBS-2 as standards for K and Th respectively. However, due to large intrinsic activity of our $\text{LaBr}_3:\text{Ce}$ crystal, we were unable to estimate the concentrations of Th and K. Next, we determined the K and Th concentrations of US-110 using a $\text{NaI}(\text{Tl})$ GRS, connected with front-end and processing electronics developed as described above. The soil sample BBS-2 (Th = 1515 ppm) was used as a Th standard in this study. As the internal radioactivity of a $\text{NaI}(\text{Tl})$ crystal is negligible in comparison to $\text{LaBr}_3:\text{Ce}$ (Figure 5), a reliable estimation of the Th and K concentrations is possible using the 1461 and 2615 keV gamma-ray lines. The Th concentration of US-110 was estimated to be ~ 11.4 ppm and is within 14% of the 13.2 ppm value determined using a HPGe GRS. The K concentration of US-110 was estimated to be 0.87%, and is within $\sim 10\%$ of the 0.78% value determined using a HPGe GRS. Estimation of U was not feasible in the present study using $\text{NaI}(\text{Tl})$ GRS due to interferences between Th and U lines and poor energy resolution of the $\text{NaI}(\text{Tl})$ detector.

The above results indicate that $\text{LaBr}_3:\text{Ce}$ detectors will not be suitable for measurements of elemental abundances of Th, U and K. However, large $2'' \times 2''$ CeBr_3 crystals have been developed recently⁶, which provide an

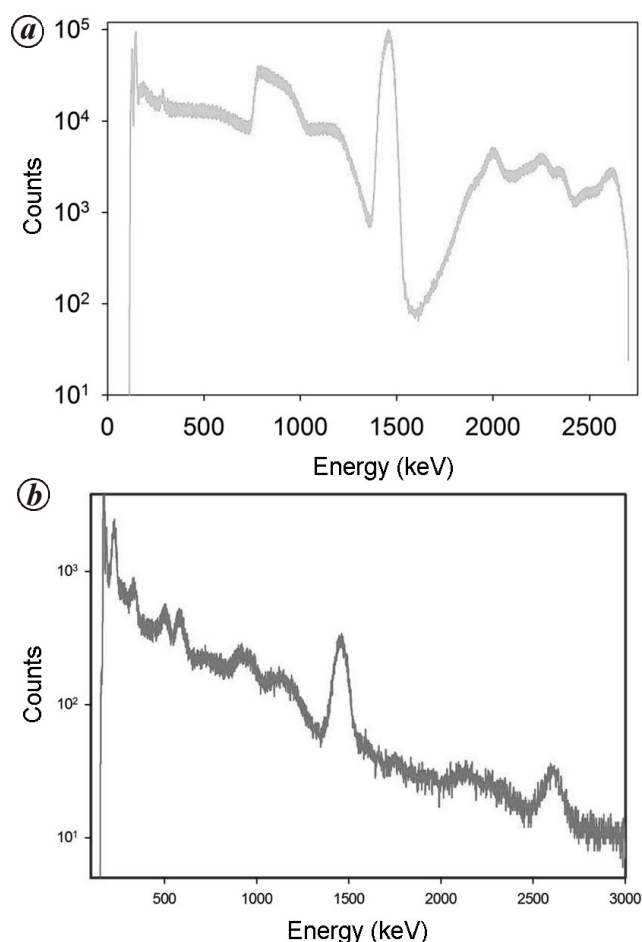


Figure 5. *a*, Background spectra obtained using the $\text{LaBr}_3:\text{Ce}$ GRS; *b*, Spectra obtained using $\text{NaI}(\text{Tl})$ GRS from the sample STD-110.

Table 1. Elemental concentrations for sample US-110 determined using HPGe and $\text{NaI}(\text{Tl})$ gamma ray spectroscopy

Element	Concentration	
	HPGe	$\text{NaI}(\text{Tl})$
K	0.78%	0.87%
Th	13.2 ppm	11.4 ppm
U	2.9 ppm	–

energy resolution of ~4% at 662 keV. Further, the intrinsic activity of these crystals between 20 keV and 3 MeV (0.02 counts/s/cm³) is much lower in comparison to LaBr₃:Ce crystals (1.24 counts/s/cm³). As the detection sensitivity of CeBr₃ is at least ten times larger than LaBr₃:Ce at 1461 and 2615 keV as reported by Quarati *et al.*⁶, determination of K and Th in meteoritic and terrestrial samples is more likely to be feasible. Future measurements will determine the sensitivity of U, Th and K using CeBr₃ and cooled HPGe detectors.

1. Goswami, J. N. *et al.*, High energy X- γ -ray spectrometer on the Chandrayaan-1 mission to the Moon. *J. Earth Syst. Sci.*, 2005, **114**, 733–738.
2. Milbrath, B. D., Choate, B. J., Fast, J. E., Hensley, W. K., Kouzes, R. T. and Schweppe, J. E., Comparison of LaBr₃:Ce and NaI(Tl) scintillators for radio-isotope identification devices. *Nucl. Instrum. Meth. Phys. Res. A*, 2007, **572**, 774–784.
3. BrillLanCe™ Scintillators Performance Summary, Saint Gobain Crystals Scintillation Products Technical Note, 2009.
4. Quarati, F. *et al.*, X-ray and gamma-ray response of a 2" \times 2" LaBr₃:Ce scintillation detector. *Nucl. Instrum. Meth. Phys. Res. A*, 2007, **574**, 115–120.
5. Shukla, A. D., Bhandari, N. and Shukla, P. N., Chemical signatures of the Permian–Triassic transitional environment in Spiti Valley, India. *Geol. Soc. Am. Spec. Pap.*, 2002, **356**, 445–453.
6. Quarati, F. G. A., Dorenbos, P., Biezen, J. van der., Owens, A., Selle, M., Parthier, L. and Schotanus, P., Scintillation and detection characteristics of high-sensitivity CeBr₃ gamma-ray spectrometers. *Nucl. Instrum. Meth. Phys. Res. A*, 2013, **729**, 596–604.

Received 6 May 2015; revised accepted 7 January 2016

doi: 10.18520/cs/v110/i11/2135-2138

The effect of meteorological events on sea surface height variations along the northwestern Persian Gulf

Mohammad Reza Khalilabadi*

Malek-Ashtar University of Technology, Shiraz, Iran

Analysing semi-hourly sea surface height (SSH) observed by tidal stations of the National Cartographic Center (NCC) of Iran at Bushehr and Kangan ports indicates de-tided SSH during January 2014. This analysis shows the impact of two meteorological events during 16–17 and 24–25 January 2014, when the northwestern part of the Persian Gulf was affected by them. During both occurrences, the de-tided SSHs at both stations were uniform, but the impact was larger at Bushehr and weaker at Kangan. The results

*e-mail: rezakhalilabadi@gmail.com

show that historical NCC sea-level data would be useful for validation of numerical models which are emerging as a major tool for storm surge warning system in the Persian Gulf.

Keywords: Cyclones, meteorological events, sea surface height (SSH), surge.

THE importance and dynamics of meteorological events (e.g. storm surges) have been discussed in the literature. These are atmospheric induced variations of the sea surface height (SSH) in coastal zones, which have a range of periods between some minutes to some days. These are long waves which are similar to astronomical tides¹. Some models and software have been designed for predicting the storm surges in coastal regions^{2–4}. In spite of many benefits of these models, there are some problems: field measurements to validate the predictive numerical models are rare because the designed instrumentation for measuring normal SSH variations, such as astronomical tides, breaks down under the onslaught of abnormally high sea level during major surges⁵.

The Persian Gulf is an important region in the Middle East situated at the northwest of the Indian Ocean. The importance of the Persian Gulf is due to huge quantities of oil and gas. The Gulf is surrounded by six countries (Iran, Iraq, Kuwait, Saudi Arabia, Qatar and the United Arab Emirates); Iran has the longest coastline of about 900 km. The Gulf generally is affected by tropical storms. There are several Iranian islands in the Persian Gulf. The most famous among them are Hormuz, Khark, Qeshm, Kish, Tonb-e-Kuchak, Tonb-e-Bozorg and Abu-Musa^{6–9}. In this communication, sea-level variations related to atmospheric pressure and wind fields at Bushehr and Kangan ports, Iran, which are situated in the northwestern region of the Persian Gulf, have been studied.

The National Cartographic Center (NCC) of Iran has established various permanent tidal stations along the northern coastlines of the Persian Gulf and the Gulf of

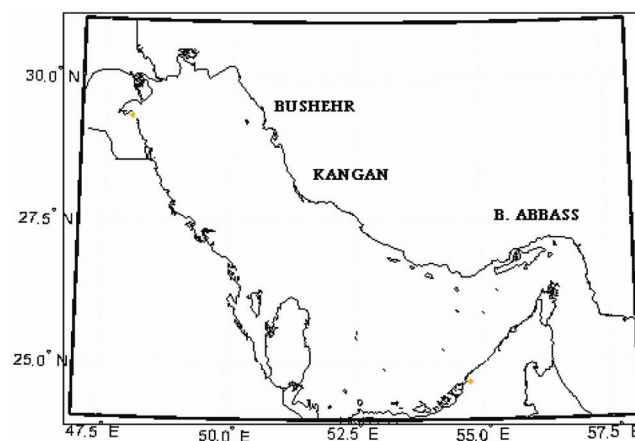


Figure 1. The study area and location of tidal stations.